Reverse annealing of boron doped polycrystalline silicon

Beop-Jong Jin[1], Won-Eui Hong[1], Jung-Yoon Lim[1], Deok Hoi Kim[2], Tstomu Uemoto[2], Chi Woo Kim[2] and Jae-Sang Ro[1]

[1]Dept. of Materials Science and Engineering, Hongik Univ. Seoul, 121-791, Korea

TEL:82-2-334-0750, e-mail: jsang@wow.hongik.ac.kr.

[2]LTPS Team, AMLCD Business, Samsung Electronics, Yongin-City, Gyeonggi-Do, 449-711, Korea

Keywords : Doping, Activation, Reverse annealing, LTPS TFTS

Abstract

Isothermal activation annealing was carried out using boron doped SLS poly-using an RTA system. We observed different behavior of reverse annealing depending on the implantation conditions.

1. Introduction

Non-mass analyzed ion shower doping (ISD) technique with a bucket-type ion source or mass-analyzed ion implantation with a ribbon beam-type has been used for source/drain doping, for LDD (lightly-doped-drain) formation, and for channel doping in fabrication of low-temperature poly-Si thin-film transistors (LTPS-TFT's) [1,2,3]. Due to thermally susceptible glass substrate the annealing temperatures for dopant activation after ion implantation are restricted to low temperatures. In contrast to semiconductor processing in which the bulk single crystalline silicon is used a very thin poly-Si on the top of a SiO_2 dielectric layer is utilized as an active layer in LTPS-TFTs. In the case of boron implantation, activation at lower temperatures is limited by the formation of boron-interstitial clusters easily formed at concentrations lower than solid solubility limit. Silicon self-interstitials generated by ion implantation tends to be supersaturated in a thin layer of poly-Si since an interface between poly-Si and a SiO_2 buffer layer on the top of the glass substrate acts like a diffusion barrier to self-interstitials. These factors would affect activation behavior significantly of ion implanted poly-Si. We reported an abnormal activation behavior in boron doped poly-Si at IDW '06 where reverse annealing, the loss of electrically active boron concentration, was found in the temperature ranges between 400℃ and 650℃ using isochronal annealing [4]. The samples treated by rapid thermal annealing (RTA) for a short time were observed to exhibit lower sheet resistance than those by furnace annealing (FA) for a long time. The reverse annealing was believed to play an important role for activation efficiency. We report here on reverse annealing behavior of boron doped SLS poly-Si using isothermal annealing.

2. Experimental

For the sample preparation SiO_2 insulation layer with a thickness of 500 nm was formed on a glass substrate of 300 mm x 400 mm x 0.7 mm (width x length x thickness) by means of plasma enhanced chemical vapor deposition (PECVD). An a-Si thin film with a thickness of 50 nm was formed successively upon the insulation layer using PECVD. Poly-Si was produced by two-shot-SLS on which 75 nm thick PECVD SiO_2 was deposited. The glass substrate was broken into pieces of 20 mm x 20 mm, thereby preparing a test piece. As indicated in Fig. 1 through doping of boron was conducted with two ion energies of 20 keV (Sample #20) and 30 keV (Sample #30), respectively at a dose of $1x10^{15}/cm^2$ using a mass-analyzed ion implanter. Isothermal activation annealing using an RTA system was conducted at 550℃, 600℃ and 650℃ from 15 to 150 sec, respectively. The sheet resistance was measured using a 4-point-probe. Activation efficiency and Hall mobility of charge carriers were determined by Hall measurement using a van der Paw method.

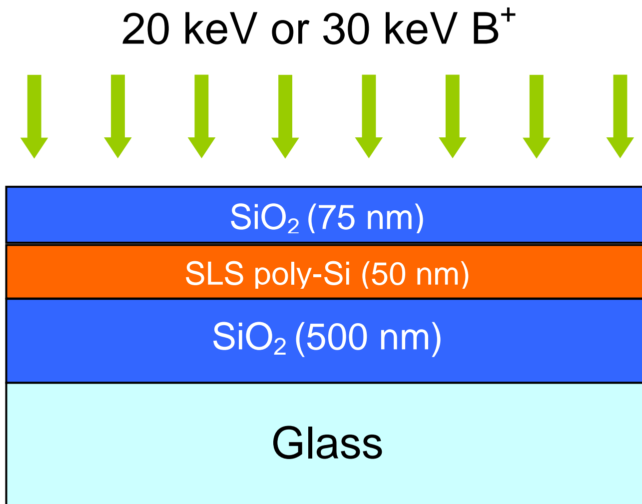

Fig. 1. Schematic diagram of implantation conditions used in this study

3. Results and discussion

Since boron implantation was conducted through 75 nm-thick SiO_2 we calculated effective dose and damage accumulated in 50 nm-thick SLS poly-Si using TRIM-code simulation. As indicated in Table 1 the effective dose for the samples implanted with 20 keV (sample #20) and 30 keV (sample #30) do not show any significant difference while the calculated defect density accumulated in poly-Si for the sample #30 has almost the double value compared to that for the sample #20.

TABLE 1. Calculated dose and damage accumulated in 50 nm-thick SLS poly-Si according to TRIM-code simulation for the samples #20 and #30, respectively.

	20 keV B^+ (Sample #20)	30 keV B^+ (Sample #30)
Effetive Dose (#/cm^2)	3.91×10^{14}	4.84×10^{14}
Defect Density (#/cm^2)	5.15×10^{16}	1.04×10^{17}

Using these two samples isothermal RTA annealing was performed at 550℃, 600℃ and 650℃ from 15 to 150 sec, respectively. Figure 2 shows changes of sheet resistance as a function of annealing time for the sample #20. The sheet resistance increases as an annealing time increases at all three temperatures. It increases gradually as a function of annealing time under the annealing conditions of 550℃ and 600℃, respectively. It, however, increases rapidly beyond 30 sec under the annealing condition of 650℃. According to Hall measurement as indicated in Fig. 3-(a) carrier concentration decreases as an annealing time increases saying that reverse annealing does occur. Meanwhile, the Hall mobility increases as an annealing time increases as shown in Fig. 3-(b). This means that as-implanted damage is recovered. Hall measurement reveals that carrier concentration decreases gradually and the Hall mobility also increases gradually under the annealing conditions of 550℃ and 600℃, respectively. However, it is interesting to note that a sudden drop of carrier concentration is closely related to a rapid increase of Hall mobility beyond 30 sec under the annealing condition of 650℃. Thus it can be said that the rate of damage recovery directly affects reverse-annealing kinetics.

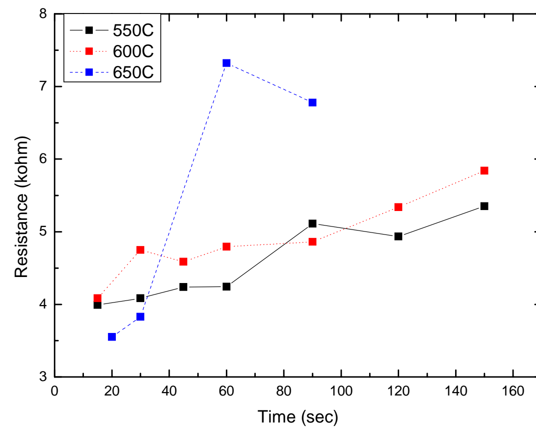

Fig. 2. Sheet resistance vs annealing time for the sample #20 annealed at 550°C, 600°C and 650°C using an RTA system

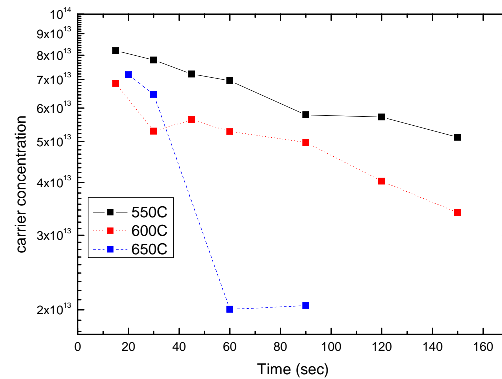

(a)

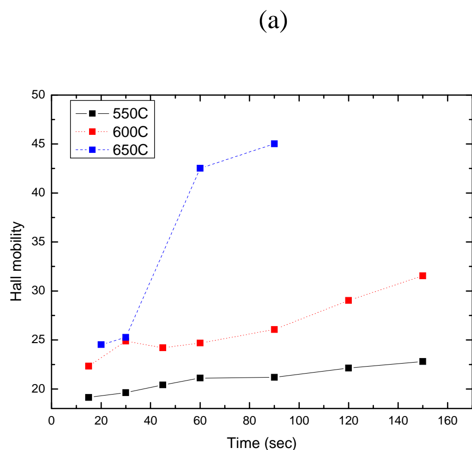

(b)

Fig. 3. (a) Carrier concentration vs annealing time and (b) mobility vs annealing time for the sample #20. RTA annealing was conducted at 550°C, 600°C, and 650°C, respectively from 15 s to 150 s.

Figure 4 shows changes of sheet resistance as a function of annealing time for the sample #30. In contrast to the case of the sample #20 the sheet resistance does not almost change as a function of annealing time under the annealing conditions of 550℃ and 600℃, respectively. It, however, increases abruptly beyond 40 sec and gradually saturates under the annealing condition of 650℃. Carrier concentration does not almost change as an annealing time increases under the annealing conditions of 550℃ and 600℃ as indicated in Fig. 5-(a). In the case of annealing at 650℃ it is quite clear that reverse annealing takes place. The Hall mobility increases weakly as a function of time under the annealing conditions of 550℃ and 600℃ while it increases significantly at 650℃ as indicated in Fig. 5-(b).

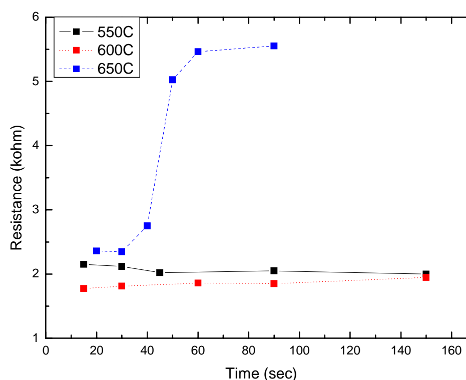

Fig. 4. Sheet resistance vs annealing time for the sample #30 annealed at 550°C, 600°C and 650°C using an RTA system.

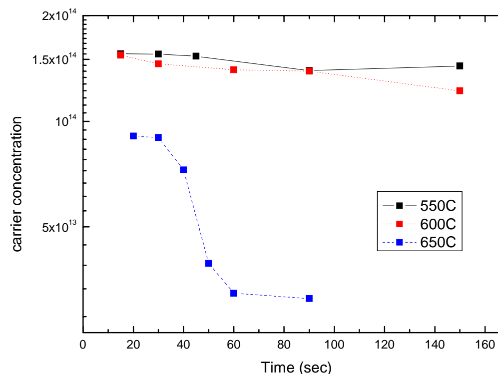

(a)

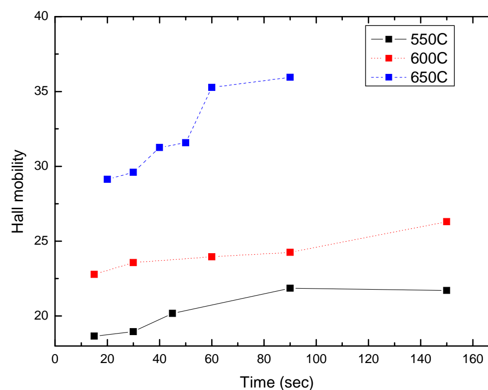

(b)

Fig. 5. (a) Carrier concentration vs annealing time and (b) mobility vs annealing time for #30 samples. RTA annealing was conducted at 550°C, 600°C, and 650°C, respectively from 15s to 150s.

Figure 6-(a) shows carrier concentration and Fig. 6-(b) shows an activation fraction as a function of annealing time for these two samples. Carrier concentration of the sample #30 is observed to be higher than that of the sample #20. One might judge that the reason is that the actual dose of the sample #30 is higher than that of the sample #20 as can be seen in Table 1. However, Fig. 6-(b) clearly tells that the activation fraction (active dose / actual dose) of the sample #30 is higher than that of the sample #20 under the annealing conditions of 550℃ and 600℃. As the annealing temperature increases to 650℃, where reverse annealing was observed to occur for these two samples, the activation fraction becomes almost the same.

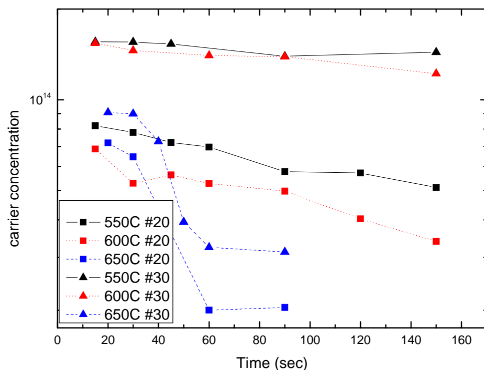

(a)

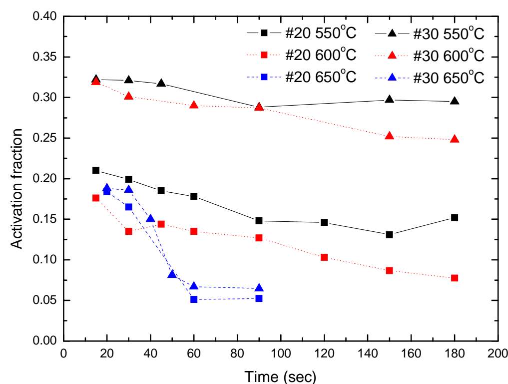

(b)

Fig. 6. (a) Carrier concentration vs annealing time and (b) activation fraction vs annealing time for the samples #20 and #30, respectively. RTA annealing was conducted at 550°C, 600°C, and 650°C, respectively from 15 s to 150s.

In this study we observed different behavior of reverse annealing in boron doped poly-Si depending on the implantation conditions. The amount of as-implanted damage seems to affect the kinetics of reverse annealing. In the case of boron doped single crystal it was observed that the degree of reverse annealing becomes larger as the amount of as-implanted damage increases [5]. In our case, however, we observed the opposite behavior. As the amount of as-implanted damage increases the kinetics of reverse annealing seems to be slower. At the present time it is not clear to understand an exact mechanism of the observed behavior in this study. Silicon self-interstitials generated in boron implanted poly-Si located on the top of SiO_2 tends to be much more supersaturated than those in boron doped single crystal. Moreover, grain boundaries may play an important role in poly-Si in contrast to the case of single crystal.

4. Summary

We observed different behavior of reverse annealing in boron doped poly-Si depending on the implantation conditions. Accumulated defect density seems to affect the kinetics of reverse annealing. These results should be well understood for better LTPS TFT processing.

5. Acknowledgment

This work was supported by Samsung Electronics Company.

6. References

1. A. Yoshida, K. Setsune, and T. Hirao, *Appl. Phys. Lett*, **51**, 252 (1987)
2. G. Kawachi, T. Aoyama, K. Miyato, Y. Ohno, A. Mimura, N. Komishi, and Y. Mochizuki, *J. Electrochem. Soc*, **137**, 3522 (1990)
3. Yasuyoshi Mishima and Michiko Takei, *J. Appl. Phys*, **75**, 4933 (1994)
4. B.-J. Jin, S.-J. Oh, D. H. Kim, T. Uemoto, C W Kim and J.-S. Ro, IDW '06 Technical Digest p 769 (2006)
5. T. E. Siedel and MacRae, in F. Eison and L. Chadderton, Eds., First Intl. Conf on Ion Implantation, 5. Thousand Oaks, Gordon and Breach, New York (1971)